Small-Net vs. Relays in a Heterogeneous Low Energy LTE Architecture

Weisi Guo, Tim O'Farrell
Department of Electronic and Electrical Engineering, University of Sheffield, United Kingdom
Email: {w.guo, t.ofarrell}@sheffield.ac.uk

***Abstract*— The paper analyzes the energy consumption impact of introducing heterogeneous elements to a homogeneous deployment. Two contrasting low energy heterogeneous architectures are investigated: small cells (Small-Nets) and wireless relays. The investigation employs a multi-cell multi-user dynamic LTE simulator and both deployments are investigated for a range of urban traffic loads. The paper shows that compared to a homogeneous baseline deployment of micro-cells, both deployments reduce the total radio network energy consumption significantly (50 to 60%). The Small-Net approach reduces energy consumption by deploying more low power cells with a macro-overlay and achieves increased network capacity by spectrum reuse. The relaying approach reduces energy consumption by deploying fewer macro-cells and increases network capacity through increasing cell-edge performance.**

A combination of deployment factors were investigated in order to find the lowest energy architecture within the heterogeneous deployments. For a range of targeted traffic loads, it was found that the lowest energy solution depends on the percentage of high mobility traffic. If the percentage of high-mobility users is below 8%, the Small-Net architecture is the lowest energy architecture. Otherwise, the wireless cell-edge relaying concept offers a greater energy reduction. The paper also presents theoretical upper-bounds on energy reduction for a fixed and changing deployment.

***Index Terms*— cellular network, heterogeneous, energy efficiency, architecture, simulation**

I. Introduction

Cellular networks have been primarily designed to meet the challenges of service quality. However, there is now increasing attention on the subject of reducing energy consumption. This is important both from a commercial profit margin point of view and from a climate change perspective. Over the past five years, the communication data volume has increased by more than a factor of 10. Approximately 0.5% (650TWh) of total world-wide energy consumption is due to wireless communications, and this is set to grow by a factor of 2 over the next decade [1]. Currently, this is equivalent to the electricity generated by roughly 35 2000MW power plants. Figure 1 shows that a small proportion of the wireless energy consumption is consumed in homes and by user equipments, whilst most of it (at least 90%) is consumed by the cellular network [2]. Within the network, the majority (75%) of this energy is consumed in the radio-access-network (RAN), which is predominantly the base-stations.

This work was supported by Mobile VCE and EPSRC.

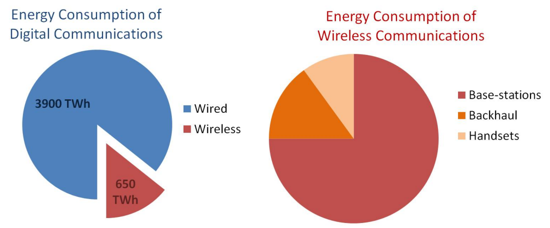

Figure 1. Energy Consumption of Wired and Wireless Digital Communications as of 2008-2010. A single UK cellular network typically consumes 40MW.

Existing deployment is a relatively flat deployment of cells, typically with a dense deployment of micro-cells in urban areas and expanding out to a sparse deployment of macro-cells in suburban and rural environments. The 3GPP standard has specified that homogeneous cells are the baseline references for performance [3]. The paper analyzes the energy consumption impact of introducing heterogeneous elements to a homogeneous deployment. A cross comparison between the heterogeneous networks is also considered.

A. Review of Challenges

Existing research has predominantly focused on specific techniques that reduce a specific aspect of cellular energy consumption. The areas considered include: deployment [4] [5] [6], scheduling [7], radio-frequency techniques [8] [9], antenna tilt [10] [11], hardware design [12], sleep mode operation [13], and multiple-access techniques [14]. However, in order to significantly reduce energy consumption in the RAN, changing the network deployment is the most promising solution [15] [16]. Thus, an integrated solution is likely to offer lower overall energy consumption.

Whilst OFDMA based Long-Term-Evolution (LTE) can significantly boost spectral efficiency compared to the existing High-Speed-Packet-Access (HSPA) network [17] [3], it remains unclear what the lowest energy deployment is. The standards define a reference and enhanced deployment of LTE micro-cells, which is shown in Fig. 2a. As shown in Fig. 2, two competing architectures have emerged from recent studies and they can be classified as:

- **Simple Small-Nets**: A dense deployment of low

doi:10.4304/jcm.7.10.716-725

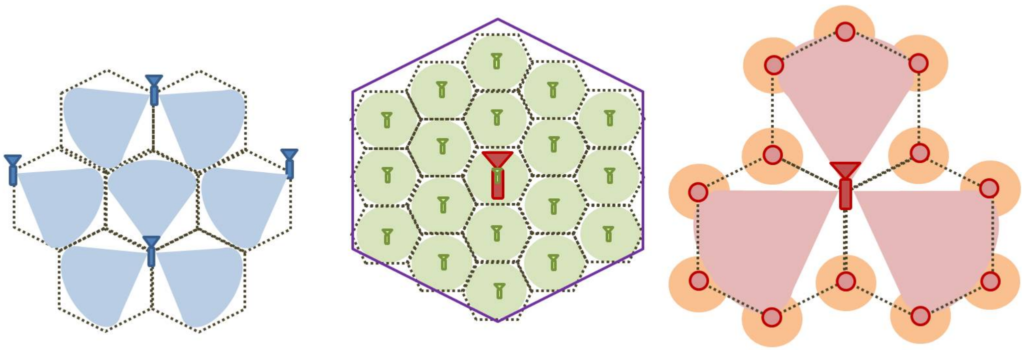

Figure 2. LTE Deployment Models: a) Reference Homogeneous Micro-Cells; b) Small-Net, and c) Macro-cells with Relays.

power pico-cells that dramatically increase network capacity by spectrum reuse, whilst consuming a low level of power [15]. The cells tend to be single-sector cell-sites with a single omni-directional antenna. A large macro-overlay is required to serve a small percentage of high mobility users. This is shown in Fig. 2b.

- **Wireless Relays**: A sparse deployment of high power macro-cells that dramatically increase network capacity by using radio techniques such as MIMO and relaying. The cells tend to be richly sectored with multiple directional antennas. The cell-edge of the large macro-cells employ low power wireless relays to improve the edge quality-of-service [18]. This is shown in Fig. 2c.

Furthermore, it remains unclear what the lowest energy configuration is within these two architecture concepts for a variety of targeted loads.

Cellular networks' downlink capacity is generally limited by interference, while the base-station (BS) energy consumption has significant elements which is overhead consumption. Many existing works share the following common assumptions:

- None or over-simplified interference modeling, leading to results that lack the principal mechanism of inter-cells interaction [6] [5] [4] [19]
- Shannon expressions (Gaussian inputs) for capacity, leading to over-optimistic performance and different optimization results [7] [19] [20]
- Transmission energy consumption only, without considering a pedestal overhead energy consumption, leading to exaggerated gains and different conclusions [21] [22] [23]

Due to the fact that cellular networks are interference limited and that the transmit power constitutes a very small proportion of the total power consumed at the cell-site, these assumptions can lead to misleading results.

B. Proposed Solutions

This paper proposes a simulation analysis that considers the following key cellular mechanisms:

- Full Interference Modeling from intra-cell and inter-cell interference. Results are taken from a central cell-site and the interference considers 18 nearest cell-sites, which has been shown to be sufficiently accurate [24].
- Adaptive Modulation and Coding schemes that capture capacity saturation effects.
- Distinct Radio-head, Over-head and Backhaul power consumption models.
- UE Mobility and realistic Antenna Patterns.

Furthermore, we also consider the overall energy reduction by deploying the low energy LTE architectures when compared to a baseline HSPA deployment. The following aspects of LTE deployment will be considered:

- Cell Density
- Sectorization and Fixed Frequency Reuse Patterns
- Multiple-Antenna Transmission
- Wireless Decode-and-Forward Relays

The purpose of this investigation is to find for a range of reliable downlink throughput values, what architecture layout can meet this load at the lowest energy consumption level. The results of this paper show that up to 55% total energy can be saved from the RAN, and the architecture solution depends on the expected amount of high mobility traffic. The paper also presents theoretical upper-bounds on energy reduction for a fixed and changing deployment.

II. SYSTEM MODEL

A. System Simulator

The paper now introduces the system simulator used to derive results. The system layer simulation results are derived from our own proprietary ***VCESIM LTE Dynamic System Simulator***, which is a proprietary LTE dynamic system simulator developed at the University of Sheffield for industrial members of the Mobile Virtual

TABLE I.
SYSTEM PARAMETERS FOR VCESIM SIMULATOR [15] [27]

LTE System Parameters		
Parameter	**Symbol**	**Value**
LTE Operating Frequency	f_{LTE}	2600MHz
LTE System Bandwidth	BW_{LTE}	5MHz, 20MHz
Subcarrier Size	BW_{sc}	15kHz
HSPA System Parameters		
HSPA Operating Frequency	f_{HSPA}	2200MHz
HSPA System Bandwidth	BW_{HSPA}	5MHz
HSPA Chip Rate	$BW_{HSPA,CR}$	3.84Mc/s
Relay Parameters		
Relay Max. Tx. Power	P_{relay}	1W
Relay Radiohead Power	$P_{relay,RH}$	10W
Relay Overhead Power	$P_{relay,OH}$	10W
Common Parameters		
Traffic Load	R_{traffc}	6-120 Mbit/s/km^2
Cell Radius	r_{cell}	200-1500m
Inter-cell-site Distance	d_{cell}	$1.5r_{cell}$
Antenna Pattern	$A(\theta)$	(1)
UE Downlink Target QoS	R_{QoS}	1Mbit/s
UE antenna Height	H_{UE}	1.5m
Cell antenna Height	H_{cell}	10-35m
Scheduler		Round Robin
Antenna Down-tilt	T	0-20 degrees
Pathloss Model	λ	WINNER II
AWGN Power	n	6×10^{-17} W
Mobility Model	$Mobility$	Brownian Motion
Traffic Load	L	Full Buffer ($L = 1$)

Centre of Excellence (MVCE). The simulator is benchmarked against 3GPP tests [3] and has been verified by our sponsors Fujitsu and Nokia Siemens Networks. The paper utilizes the appropriate WINNER urban pathloss models, which includes path-loss, multipath and shadow fading models [25] [26]. The list of system modelling variables is given in Table I.

In the case when the cell-sites have a single omni-directional antenna, the antenna gain is unity. In the case when the cell-sites each have 3 or 6 horizontal sectors, the antenna gain (dB) is:

$$A_{cell}(\theta) = A_{bs} - \min[12(\frac{\theta}{\theta_{3dB}})^2, A_m], \quad (1)$$

for an angle θ_a from the azimuth or elevation plane. For 3 sectors: $A_{bs} = 17.6dBi$ is the bore-sight gain, $A_m = 20dBi$, and $\theta_{3dB} = 75$ degrees in azimuth and $\theta_{3dB} = 20$ degrees in elevation. For 6 sectors: $A_{bs} = 23.4dBi$, $A_m = 25dBi$, and $\theta_{3dB} = 60$ degrees in azimuth and $\theta_{3dB} = 20$ degrees in elevation.

B. Link Level Capacity

The recommended deployment in 3GPP LTE is that all cell-sites (BS) are co-frequency. In simulations, each BS's throughput considers interference from 2 additional tiers of BS, which is sufficiently accurate compared to a higher number of tiers for both homogeneous and heterogeneous deployments [24]. The instantaneous received signal to interference plus noise ratio (SINR) of a single sub-carrier (s) of a single user that is attached to BS i is:

$$\gamma_{s,i} = \frac{|h_i|^2 \lambda_i 10^{\frac{\mathcal{S}_i + A(\theta_i)}{10}} P_{s,i}}{n + \sum_{j=1, j\neq i}^{N_{cell}} |h_j|^2 \lambda_j 10^{\frac{\mathcal{S}_j + A(\theta_j)}{10}} P_{s,j}}, \quad (2)$$

where P is the transmit power of BS, λ is the pathloss, n is the AWGN power per sub-carrier and A is the antenna gain. The interference term considers the transmission power from 18 other nearest co-frequency cell-sites and this is sufficiently accurate as shown in [24]. A similar expression can be obtained for HSPA. The value of each parameter is given in Table I.

Log-normal shadow fading is defined as $\mathcal{S} = \mathcal{N}(0, \sigma_s^2)$, where σ_s^2 is the variance of the shadow fading. The multipath fading gain is defined as: $h \sim \mathcal{N}(0, 1)$ is the zero-mean unit-variance circular-symmetric complex fading coefficient. The paper employs the appropriate adaptive modulation and coding scheme given by internal link level simulators and verified against [28]. The pathloss component can be expressed as a function of the distance x: $\lambda = Kx^{-\alpha}$; where K is the frequency dependent pathloss constant and α is the pathloss exponent.

From Fig. 3a it can be seen that the adaptive modulation and coding (AMC) scheme produces a capacity relationship that is significantly different to the Shannon expression (Gaussian inputs). Whilst some existing literature employ the Shannon expression with LTE backoff adjustments (3), the throughput differences are still significant. This can have a significant impact on the system level results, with Shannon expression likely to yield different degrees of over optimistic performances at different SINR levels. The adjusted Shannon expression is as follows:

$$\mathrm{R}_{\text{Adjusted}} = \min(\log_2(1 + \frac{\gamma_{s,k}}{F}), S), \quad (3)$$

where F is the adjustment factor given as 1.5 for LTE and 2 for HSPA, derived from [16] [17]. The spectral efficiency saturation S levels are 4.32 bit/s/Hz (64-QAM Turbo 6/7) and 3.30 bit/s/Hz (64-QAM Turbo 3/4) for LTE and HSPA, respectively.

III. ENERGY METRICS

A. Power Consumption

A general cell-site power consumption model can be broken down into a power dependent and power independent parts. For a cell-site with N_K sectors and N_A transmit antennas per sector, the power consumption is:

$$P_{\text{OP,cell}} = N_K N_A (\frac{P}{\mu} + P_{\text{OH}}), \quad (4)$$

where P is the transmit power, μ is the radio-head efficiency, P_{OH} is the overhead power consumption, which includes the backhaul power consumption. The power consumption of different cell sizes is presented in Fig. 3b, with data taken from [29] and interpolation is used to fill missing cell-sizes.

B. Energy Consumption

The paper consider a RAN with users demanding a traffic load of M bits of data over a finite time duration

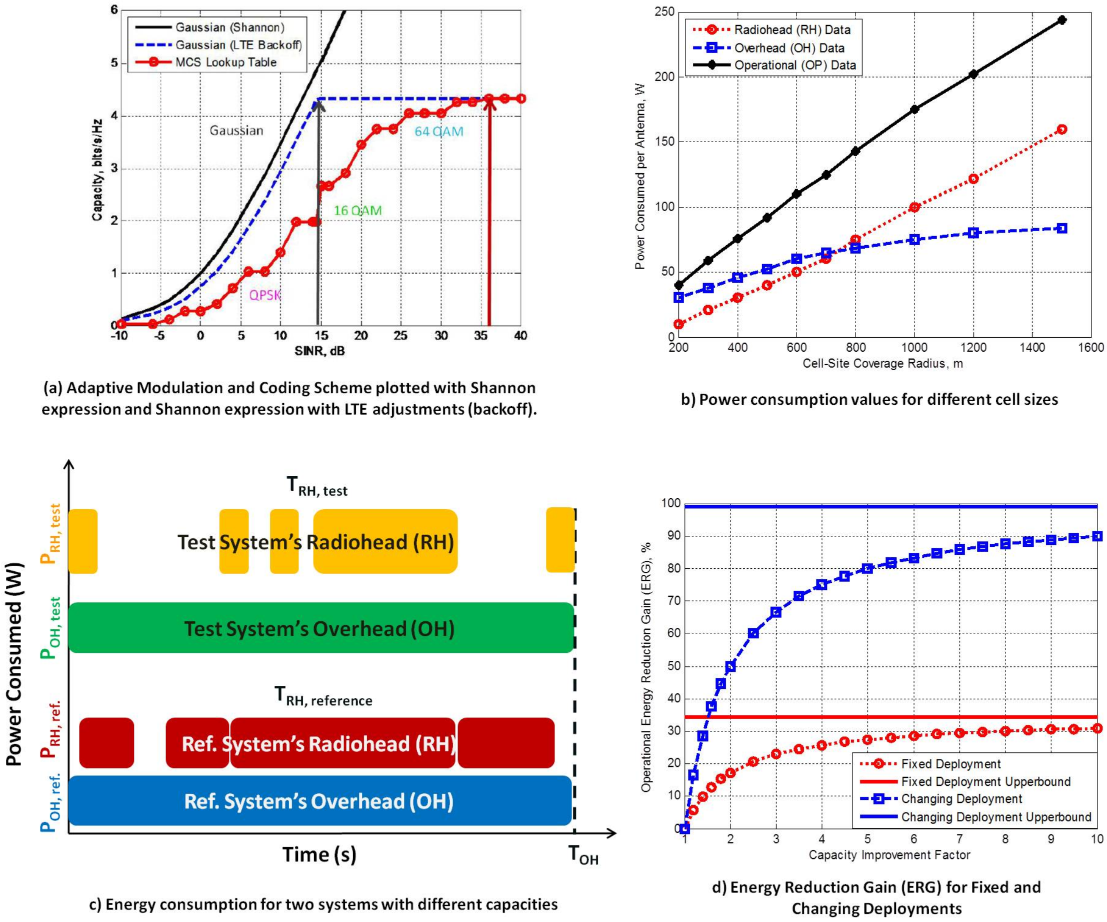

(a) Adaptive Modulation and Coding Scheme plotted with Shannon expression and Shannon expression with LTE adjustments (backoff).

b) Power consumption values for different cell sizes

c) Energy consumption for two systems with different capacities

d) Energy Reduction Gain (ERG) for Fixed and Changing Deployments

Figure 3. a) Link Level Capacity; b) Total power consumption variation with cell size [29]; c) Energy consumption for reference and test system; d) Energy Reduction Gain (ERG) for a Fixed and Changing deployment.

(T_{OH}), as shown in Fig. 3c. The offered traffic rate is $R_{\text{traffic}} = M/T_{\text{OH}}$. Two networks are considered:

- *Reference Network* can achieve a throughput of $R_{\text{RAN,ref.}}$ with $N_{\text{ref.}}$ cell-sites deployed.
- *Test Network* can achieve a throughput of $R_{\text{RAN,test}}$ with N_{test} cell-sites deployed.

Both of the network's throughput R_{RAN} exceeds the offered traffic load R_{traffic}. Due to the fact that the reference and the test system might have different capacities and scheduling mechanisms, the duration which the radiohead spends in transmitting ($T_{\text{RH}} = M/R_{\text{RAN}}$) is different for the two systems. Fig. 3c shows the comparison of two systems and illustrates a common overhead time of operation, but different radiohead transmission times.

The energy consumed by a cell over a period of T_{OH}, where the cell has transmitted over a period of T_{RH} is:

$$\text{E}_{\text{OP,cell}} = N_K N_A (\frac{P}{\mu} T_{\text{RH}} + P_{\text{OH}} T_{\text{OH}}), \quad (5)$$

where the term P_{OH} includes the backhaul power.

In order to compare the energy consumption of different systems, a relative notion of transmission duration and operational duration must be defined. A useful metric is the Energy Reduction Gain (ERG), which is the *energy saved* when a test system is compared with a reference system:

$$\begin{aligned} \text{ERG}_{\text{OP,RAN}} &= 1 - \frac{E_{\text{OP,RAN,test}}}{E_{\text{OP,RAN,ref.}}} \\ &= 1 - \frac{\sum_m^{N_{\text{test}}} (P_{m,\text{RH}} T_{m,\text{RH}} + P_{m,\text{OH}} T_{m,\text{OH}})}{\sum_n^{N_{\text{ref}}} (P_{n,\text{RH}} T_{n,\text{RH}} + P_{n,\text{OH}} T_{n,\text{OH}})} \\ &= 1 - \frac{\sum_m^{N_{\text{test}}} (P_{m,\text{RH}} \frac{R_{\text{traffic}}}{R_{\text{RAN,test}}} + P_{m,\text{OH}})}{\sum_n^{N_{\text{ref.}}} (P_{n,\text{RH}} \frac{R_{\text{traffic}}}{R_{\text{RAN,ref.}}} + P_{n,\text{OH}})}. \end{aligned} \quad (6)$$

C. Transmission Efficiency

The term $\frac{P^{\text{RH}}}{R_{\text{RAN}}}$ in (6) is an indication of the average radio transmission efficiency, which does not consider the overhead energy. This is commonly used to measure energy consumption in the literature [21], and is known as the Energy-Consumption-Ratio (ECR). This shows how the operational energy saving can encompass existing energy metrics that only consider transmission efficiency.

D. Energy Reduction Upper-Bounds

For a reference and test system that employ the same cell deployment, this section considers how much energy can be saved by improving the capacity of the system. Assuming that the capacity of the test system ($R_{\text{RAN,test}}$) was improved to an arbitrarily large value so that $\frac{R_{\text{traffic}}}{R_{\text{RAN,test}}} \sim 0$. The resulting energy reduction that can be achieved from (6) is therefore:

$$\text{ERG}_{\text{RAN,fixed}} = 1 - \frac{\sum_m^{N_{\text{test}}} P_{m,\text{OH}}}{\sum_n^{N_{\text{ref.}}} (P_{n,\text{RH}} \frac{R_{\text{traffic}}}{R_{\text{RAN,ref.}}} + P_{n,\text{OH}})}. \quad (7)$$

That is to say, given the cell-site power consumption values presented in Fig. 3b and the backhaul consumption, only 35 to 40% operational energy reduction gain can be achieved. The results for different capacity improvements are shown in Fig. 3d.

In the **Fixed Deployment** scenario, the location and number of cell-sites do not change. The capacity of each cell-site is improved so that the ERG relationship (6) is improved by letting the ratio between test system's throughput and offered traffic load converge to 0 ($\frac{R_{\text{traffic}}}{R_{\text{RAN,test}}} \rightarrow 0$). In reality the capacity improvement achieved by a single technique is significantly less than the upper-bound and in order to increase the energy saving, a redeployment is needed. This is why the RAN architecture plays a significant role in reducing energy consumption.

In the **Changing Deployment** scenario, the location and number of cell-sites can change, as well as the capacity of each cell-site. In so doing, the ERG relationship (6) is improved by letting the power consumption of the test RAN converge to an arbitrarily small number so that the ERG can approach:

$$\text{ERG}_{\text{RAN,changing}} \rightarrow 1. \quad (8)$$

That is to say, an energy reduction that tends to 100% can be achieved in theory. The results for different capacity improvements are shown in Fig. 3d. The changing deployment relationship is derived from (6) by letting the energy consumption of the test system converge to a small number ($E_{\text{RAN,OP,test}} \rightarrow 0$). This can be achieved by deploying many low power cells or fewer high power cells. In practice, this is not possible without a significant improvement in bandwidth and energy harvesting techniques. Nonetheless, for a given capacity improvement, the potential energy reduction by changing the network deployment far exceeds that achieved by a fixed deployment that adapts energy saving techniques only.

The ERG expression in (6) shows that there are load dependent (RH) and load independent elements (OH). By removing the load independent elements, the whole ERG expression becomes load dependent. In changing deployment, the number of cells can change, and an improvement in capacity affects the total power consumption. Therefore, every component has become load dependent. Therefore, the changing deployment plot also corresponds with the concept of the ERG is without load independent consumption (OH).

The bounds derived in this section are asymptotic upper-bounds. Whilst the energy saving gains for fixed deployment is limited, changing the deployment is a costly exercise with many practical issues relating to site leasing. The paper now considers the performance of 3GPP reference deployment architectures and how they can be improved with heterogeneous elements.

IV. HOMOGENEOUS ARCHITECTURES

A. Reference Deployment and Results

The paper first outlines the **reference** homogeneous cell deployment architecture for HSPA and LTE as specified in 3GPP standards [3] [26]. It has the following setup, as shown in Fig. 2a:

- Each micro cell-site has 3 horizontal sectors using a directional antenna (1).
- Frequency Reuse Pattern 1.
- SISO Transmission is employed in the reference scenario.

This is used as a reference baseline, because the co-frequency symmetrical coverage pattern yields better results than other patterns [30].

The capacity and power consumption of the RAN can be increased by increasing the density of cells deployed in a given area. Note that as the number of cells per unit area increases, the effective cell coverage size is reduced and the power consumption model also changes in accordance with Fig. 3b.

The plots in Fig. 4 show the following key throughput performance results:

- The achievable downlink throughput saturates as the cell size decreases to smaller than a radius of 200m (ISD: 300m). This is due to the fact that at small distances, the chance that interfering cells are also in line-of-sight increases and the level of interference dramatically.
- LTE is on average 60 to 70% spectrally more efficient than HSPA. Given the fact that LTE bandwidth can be 20MHz, the increased resulting average throughput is up to 5 folds higher.

As previously discussed, in order to reduce energy consumption, there are two methods, namely: fixed deployment, increase the capacity; or fixed capacity, change the deployment.

Using the results shown in Fig. 4b, the following energy reduction gains can be achieved:

- **Fixed Deployment:** For a given deployment with a given operational power consumption level, LTE can reduce energy consumption: 17% (5MHz) and 28% (20MHz) when compared with a 5MHz HSPA deployment.
- **Changing Deployment:** For a given RAN throughput that both systems can achieve, LTE can reduce energy consumption: 40% (5MHz) and 80%

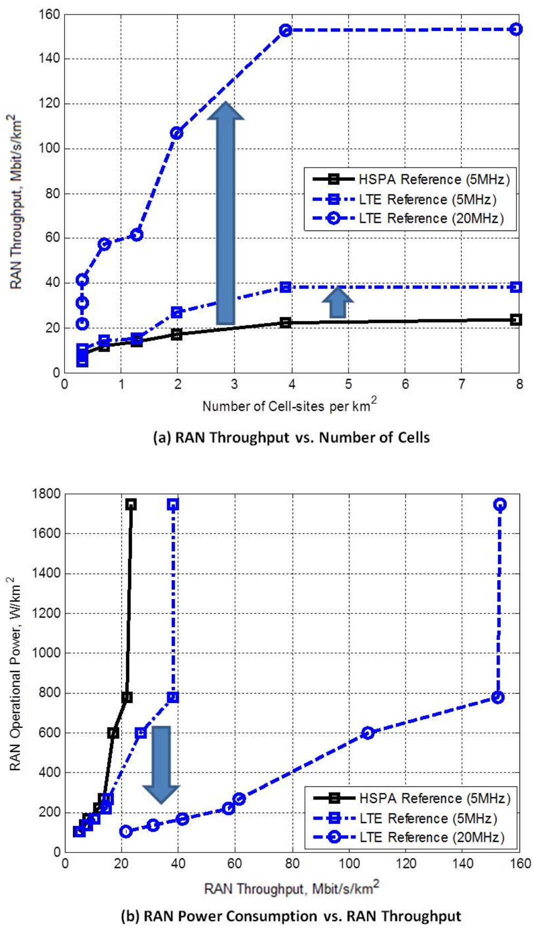

Figure 4. HSPA and LTE Reference Deployments: a) RAN Throughput vs. Number of Cells; b) RAN Power Consumption vs. RAN Throughput.

(20MHz) when compared with a 5MHz HSPA deployment.

Clearly, if each cell can achieve a higher capacity, then reducing the cell density (changing deployment) yields a much higher energy reduction gain. Whether, this is a realistic operational solution is beyond the scope of this paper and is a future research area.

B. Enhanced Deployment and Results

The paper now outlines the **enhanced** homogeneous cell deployment architecture, which has the following setup, as shown in Fig. 2a:

- Each cell-site has 3 to 6 horizontal sectors using a directional antenna (1) with Frequency Reuse Pattern 3.
- SISO or SIMO (1x2 Maximum-Ratio-Combining (MRC)) or MIMO (2x2 Space-Frequency-Block-Coding (SFBC)) transmission

In order to achieve the same RAN throughput as the reference deployment, fewer high power large cells are required per unit area. The results in Fig. 5 show that for throughput from low to high (40 to 110 Mbit/s/km^2), the 6 Sector Frequency Reuse 3 deployment (6SF3) has

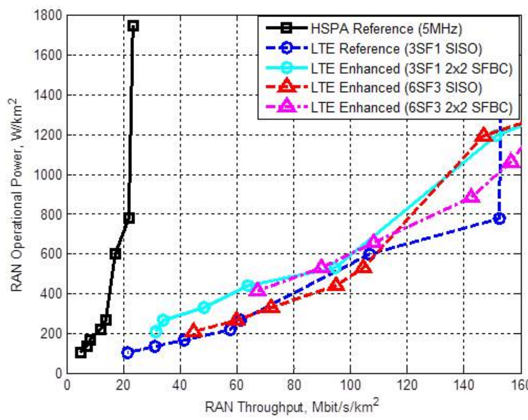

Figure 5. HSPA and LTE Reference and Enhanced Deployments for RAN Power Consumption vs. RAN Throughput.

a similar energy efficiency to the reference deployment. The results show that SISO deployment is preferred to MIMO, because the additional energy consumption of MIMO doesn't outweigh the improvements in spectral efficiency. Given that SIMO doesn't require any additional energy expenditure on the BS end, it can be reasoned that SIMO transmission is preferred if available. This is proven to be true in Fig. 7b for omni-directional cells.

V. Heterogeneous Wireless Relay Architecture

A. Deployment

The paper now outlines the Het-Net cell with relays architecture, which has the following setup, as shown in Fig. 2b:

- Each cell-site has 3 to 6 horizontal sectors using a directional antenna (1) with Frequency Reuse Pattern 3.
- SISO or SIMO (1x2 Maximum-Ratio-Combining (MRC)) or MIMO (2x2 Space-Frequency-Block-Coding (SFBC)) transmission
- Decode-and-Forward wireless relays are deployed at the cell-site edge. Each wireless relay is an omni-directional low power relay. The relays employ either co-frequency or non-co-frequency transmission on all channels.

The paper considers Decode-and-Forward (DF) wireless relays. The throughput of the relay-UE channel is limited by the minimum of the rate between the cell-relay and relay-UE channel [31]:

$$R_{\text{relay}} = \min(R_{\text{cell-relay}}, R_{\text{relay-UE}}). \quad (9)$$

That is to say, in order for relays to improve the performance of cell-edge UEs, the cell-relay channel needs to be considered. The following types of relays are considered:

- In **Co-Frequency (CF) Relaying**, all the relay and non-relay channels share the same bandwidth and cause mutual interference.

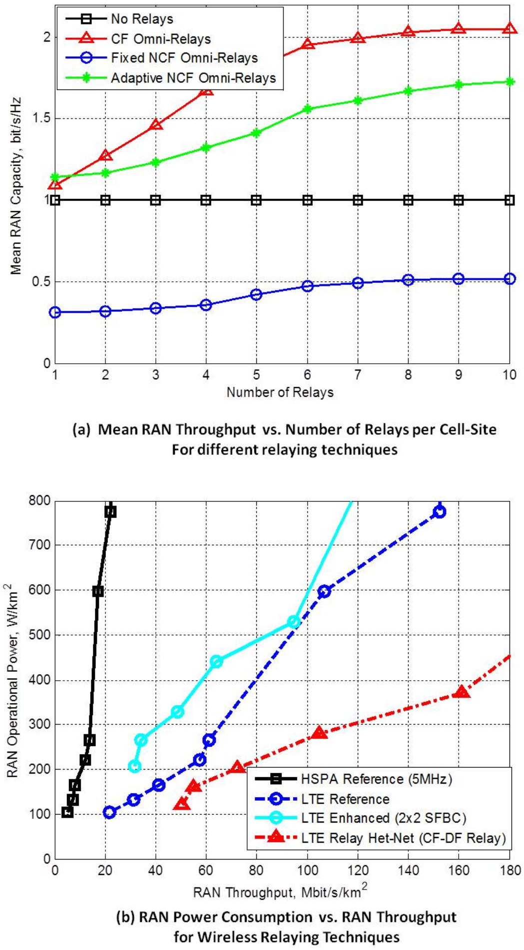

Figure 6. a) Mean RAN Spectral Efficiency vs. Number of Relays per Cell-Site; b) RAN Power Consumption vs. RAN Throughput results for Reference, Small-Net and Relay deployments.

- In **Fixed Non-Co-Frequency (F-NCF) Relaying**, the problem formulation is conceptually the same as co-frequency (CF) relay deployment except the interference and bands available is different. The cell-UE channels employ a set of frequency bands and the relay channels operate on a different set of frequency bands. The amount of bandwidth allocated to the relay channels is fixed to a certain value, and not adaptive to the position of the UE being served.
- In **Adaptive Non-Co-Frequency (A-NCF) Relaying**, the number of resource blocks allocated between the relay channels is adapted on a per user basis without considering fading variations. That is to say, given a particular user position, the relay capacity is ensured so that the cell-relay channel and relay-user channel is equal ($R_{\text{cell-relay}} = R_{\text{relay-UE}}$).

Given that the relays are deployed on the cell edge of existing cell-sites, in order to improve the UE's performance at the cell-edge, the cell-relay channel would need to be better than the cell-UE channel. The paper employs an improved cell-relay channel of 5dB, which can be achieved by increasing relay receiver sensitivity or directional transmissions between the cell and relay. The relays transmit at a power of 1W and have an overall power consumption value of 20W.

B. Relaying Results

The results in Fig. 6a show that as the number of relays per cell-site increases, the spectral efficiency improvement saturates. For co-frequency relaying, which offers the greatest improvement, the saturation point is approximately 6 relays per cell-site. Furthermore, the results show that Co-Frequency relaying benefits the RAN more than both Non-Co-Frequency techniques. This is due to the fact that whilst the CF relays create new cell-edge zones within the cell deployment, the new cell edges have are less severe (a greater SINR value). Therefore, the relaying Het-Net will employ 6 CF DF wireless relays, and its performance will be compared with the reference HSPA and LTE system, as well as the Small-Net architecture.

Using the results shown in Fig. 6b, the following energy reduction gains can be achieved when the relaying Het-Net is compared against the following reference systems:

- **HSPA Reference:** at least 80% ERG can be achieved compared to a 5MHz HSPA reference deployment, and 72% ERG can be achieved compared to a 20MHz HSPA deployment.
- **LTE Reference:** 25 to 55% ERG can be achieved compared to a 20MHz LTE reference deployment.

The paper now considers an alternative Small-Nets heterogeneous deployment and compares its performance for a variety of traffic loads with the relaying architecture.

VI. Heterogeneous Small-Nets Architecture

A. Deployment

The paper now outlines the Small-Net cell deployment architecture, which has the following setup, as shown in Fig. 2b:

- Homogeneous underlay of pico-cell-sites, each with 1 sector using an omni-directional antenna employing Frequency Reuse Pattern 1
- SISO or SIMO (1x2 Maximum-Ratio-Combining (MRC)) or MIMO (2x2 Space-Frequency-Block-Coding (SFBC)) transmission
- Macro-cell overlay to handle high mobility users.

The capacity and power consumption of the Small-Net network can be increased by increasing the density of cells deployed in a given area. In order to achieve the same average throughput as the reference deployment, typically more low power small cells are required per unit area. For example, referring to Fig. 7a, in order to achieve a RAN throughput of 100Mbit/s/km^2, the reference deployment requires 2 cell-sites and the Small-Net requires at least 3 cell-sites per square km.

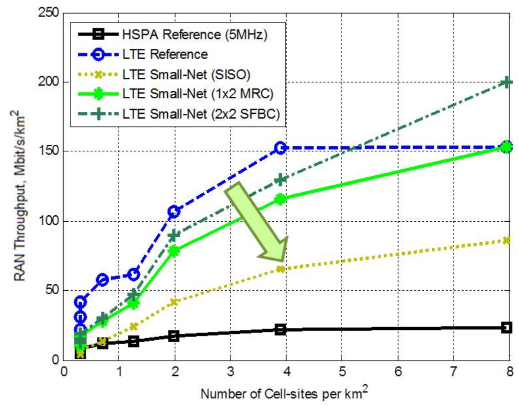

(a) RAN Throughput vs. Number of Cells

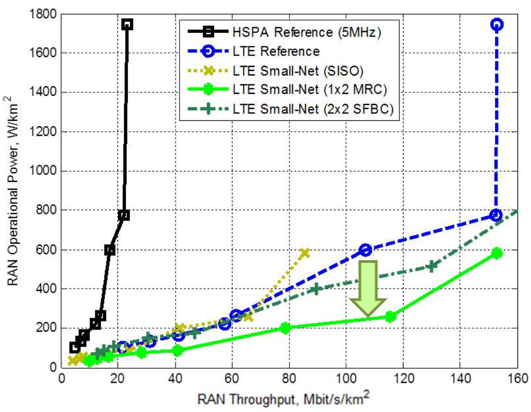

(b) RAN Power Consumption vs. RAN Throughput

Figure 7. HSPA, LTE Reference Deployments and LTE Small-Net Deployment: a) RAN Throughput vs. Number of Cells; b) RAN Power Consumption vs. RAN Throughput.

B. Small-Net Results

The plots in Fig. 7 show the following key throughput performance results **without** considering the macro-overlay:

- As the density of cells deployed increases, the achievable downlink throughput saturates slower with Small-Nets than with the reference sectorized deployment. Reason being is that interference is less significant at small distances when antenna directionality is not employed in the Small-Net cells.
- SIMO is the most energy efficient deployment when compared with SISO and MIMO, as shown in Fig. 7b. Therefore, SIMO is considered as the preferred low energy deployment solution in Small-Nets.

Using the results shown in Fig. 7b, the following energy reduction gains can be achieved against the following reference systems:

- **HSPA Reference:** 78% ERG can be achieved compared to a 5MHz HSPA reference deployment, and 67% ERG can be achieved compared to a 20MHz HSPA deployment.
- **LTE Reference:** 61% ERG can be achieved compared to a 20MHz LTE reference deployment.

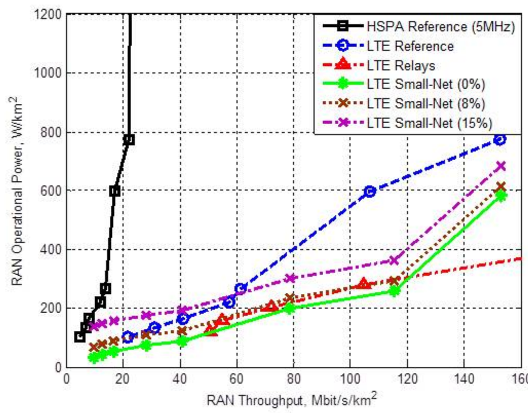

Figure 8. RAN Power Consumption vs. RAN Throughput results for: Reference, Small-Net and Relaying Het-Net with varying percentage of high mobility traffic load.

If the energy consumption of the macro-overlay is neglected, the conclusion in Small-Net deployment is that by reducing the cell-size by a factor of 50% and removing sectorization, the energy reduction gain can reach approximately 60%.

The challenges to Small-Nets include how to handover UEs with a high mobility speed (40 km/hour). To solve this problem, one or several larger macro-cells are needed to provide coverage to high mobility users. The paper considers a certain percentage of network traffic that is of high mobility and passed-off to the co-frequency macro-cell overlay. As the percentage of traffic that is passed off increases, the macro-cell power consumption increases through increased sectorization. The paper considers three traffic profiles, when 2%, 8% and 15% of the UEs are of high-mobility. When only 2% or less of the traffic is of high mobility, the excessive handovers in the Small-Net architecture causes outage for the UEs and this is accepted as within the 5% UEs that are denied Quality-of-Service. For a single sector macro-cell overlay, up to 10 Mbit/s/km^2 of the traffic can be handed-off to the macro-overlay, which equates to 8% of the high traffic load. For a tri-sector macro-cell overlay, up to 20 Mbit/s/km^2 of the traffic can be handed-off to the macro-overlay, which equates to 15% of the high traffic load. It was found that the Small-Net and Relaying architectures offer almost identical energy consumption vs. throughput relationships for the 8% scenario, as shown in Fig. 8. As the percentage of highly mobile users increases, the Small-Net becomes a less beneficial architecture.

VII. Discussions

This paper has considered two deployment concepts, that of Small-Nets and Relaying Het-Nets. Small-Nets employ a dense deployment of single antenna pico-cells, typically of 300m inter-cell-site distance and consume

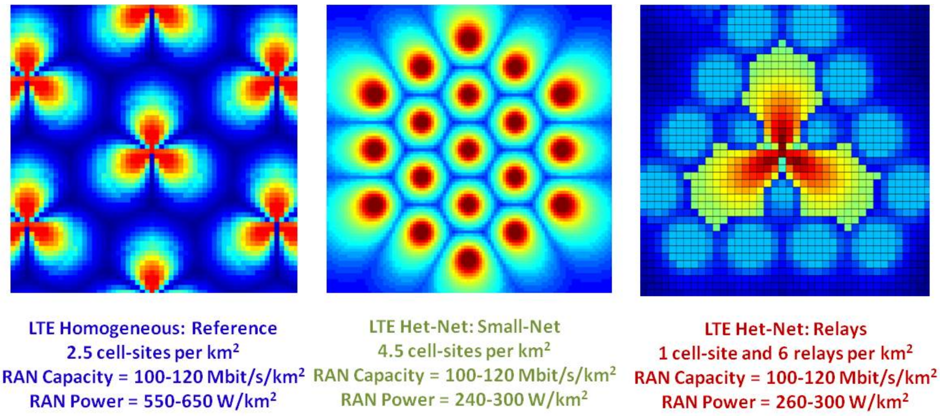

Figure 9. LTE Deployment Models: Reference, Small-Net, and Relaying Het-Net.

90W per cell-site (including 50W backhaul). They can achieve a high RAN throughput (100-120 Mbit/s/km^2) for a relatively low RAN power consumption level (240-300 W/km^2). On the other hand, relaying architecture employs a sparse deployment of multi-sector macro-cells with cell-edge relays, typically of 1500m inter-cell-site distance and 720W per cell-site (including relays and backhaul). They can achieve a high RAN throughput (100-120 Mbit/s/km^2) for a relatively low RAN power consumption level (260-300 W/km^2). The results are shown in Fig. 9.

When a negligible percentage of the traffic is highly mobile (2% or less), the Small-Net solution doesn't require any significant macro-overlay and yields the greatest energy reduction. As this percentage increases to 8%, the relaying Het-Net becomes a more favorable architecture in terms of energy reduction. Therefore, an urban environment where all the users move at pedestrian speeds should employ a dense deployment of 200m pico-cells with at most a single sector macro-overlay of 2000m in coverage size. An urban environment that have at least 8% of users moving in vehicles should deploy several 1000m macro-cells with 6 to 9 co-frequency low power relays per cell-site on the cell-edge.

This paper has also assumed that the backhaul power consumption has a constant value of 50W, irrespective of the cell size. The issue with backhaul is that the power consumption is an external factor that does not scale with cell size or technology. Should the power consumption scale down with smaller cells, this would significantly enhance the Small-Net deployment energy savings. Furthermore, there are several other modeling aspects which can change the conclusions drawn. Previous work [15] has shown that the power consumption model of cell's radiohead and the pathloss model yields the greatest impact on the energy reduction values. Moreover, how the power consumption of cells and the backhaul vary with cell size and transmission load remains unclear.

VIII. Conclusion

The results in this paper have shown that for an urban environment, the lowest energy architecture depends on the percentage of traffic that is of high mobility. For a low percentage (less than 8%), the lowest energy architecture is the Small-Net solution with a macro-cell overlay that handles the high-mobility users. For a percentage greater than 8%, the lowest energy architecture is the Relaying Het-Net solution with comprises of several macro-cells that employ co-frequency decode-and-forward wireless relays at the cell-edge. The achievable energy reduction from deploying either the Small-Net or Relaying Het-Net is approximately 55% when compared with the 20MHz LTE reference deployment, and 80% when compared with the 5MHz HSPA reference deployment.

Acknowledgment

The work papered in this paper has formed part of the Green Radio Core 5 Research Programme of the Virtual Centre of Excellence in Mobile and Personal Communications, Mobile VCE. The authors would like to acknowledge Simon Fletcher of NEC Europe, Imran Ashraf of Alcatel Lucent, John Turk of Vodafone, Yan Chen of Huawei, and Rajni Agarwal of Fujitsu UK. Fully detailed technical papers on this research are available to Industrial Members of the Mobile VCE. www.mobilevce.com

References

[1] G. Fettweis and E. Zimmermann, "ICT Energy Consumption - Trends and Challenges," in *Proc. IEEE Wireless Personal Multimedia Communications*, Finland, Sept. 2008.

[2] R. Rinaldi and G. Veca, "The hydrogen for base radio stations," in *Proc. of 29th International Telecommunication Energy Conference (INTELEC)*, Rome, Italy, 2007, pp. 288–292.

[3] Ericsson, "Summary of Downlink Performance Evaluation," 3GPP TSG RAN R1-072444," Technical Report, May 2007.

[4] C. Xiong, G. Li, S. Zhang, Y. Chen, and S. Xu, "Energy-and spectral- efficiency tradeoff in downlink OFDMA networks," in *Wireless Communications, IEEE Transactions on*, vol. 10, no. 11, Nov. 2011, pp. 3874–3885.

[5] F. Heliot, O. Onireti, and M. Imran, “An Accurate Closed-Form Approximation of the Energy Efficiency-Spectral Efficiency Trade-off over the MIMO Rayleigh Fading Channel,” in *Communications Workshops (ICC), 2011 IEEE International Conference on*, June 2011.
[6] Y. Chen, S. Zhang, S. Xu, and G. Li, “Fundamental trade-offs on green wireless networks,” in *Communications Magazine, IEEE*, vol. 49, no. 6, June 2011.
[7] S. Videv and H. Haas, “Energy-Efficient Scheduling and Bandwidth – Energy Efficiency Trade-Off with Variable Load in LTE,” in *IEEE International Conference on Communications (ICC)*, June 2011.
[8] P. Marsch and G. Fettweis, “On uplink network MIMO under a constrained backhaul and imperfect channel knowledge,” in *IEEE International Conference on Communications (ICC)*, Dresden, Germany, June 2009.
[9] O. Yilmaz, S. Hamalainen, and J. Hamalainen, “System level analysis of vertical sectorization for 3GPP LTE,” in *IEEE International Symposium on Wireless Communication Systems (ISWCS)*, Oct. 2009, pp. 453–457.
[10] J. Niemela, T. Isotalo, and J. Lempiainen, “Optimum antenna downtilt angles for macrocellular WCDMA network,” in *EURASIP Journal of Wireless Communications Networking*, 2005, pp. 816–827.
[11] D. H. Kim, D. D. Lee, H. Kim, and K. Whang, “Capacity analysis of macro/mircocellular CDMA with power radio control and tilted antennas,” in *IEEE Transactions on Vehicular Technology*, Jan. 2000, pp. 34–42.
[12] K. Mimis, K. Morris, and J. McGeehan, “A 2GHz GaN class J Power Amplifier for Basestation Applications,” in *IEEE Symp. for Radio and Wireless (RWS)*, Phoenix, USA, Jan. 2011.
[13] H. Claussen, L. Ho, and F.Pivit, “Dynamic idle mode procedures for femtocells,” in *Telecom Journal of Australia*, 2009, pp. 401–418.
[14] M. Deruyck, W. Vereecken, E. Tanghe, W. Joseph, M. Pickavet, L. Martens, and P. Demeester, “Comparison of power consumption of mobile WiMAX, HSPA and LTE access networks,” in *IEEE Conference on Telecommunications Internet and Media Techno Economics (CTTE)*, June 2010, pp. 1–7.
[15] W. Guo and T. O’Farrell, “Green cellular network: Deployment solutions, sensitivity and tradeoffs,” in *Wireless Advanced (WiAd), IEEE Proc.*, London, UK, June 2011.
[16] P. Mogensen, W. Na, I. Kovacs, F. Frederiksen, A. Pokhariyal, K. Pedersen, T. Kolding, K. Hugl, and M. Kuusela, “LTE Capacity Compared to the Shannon Bound,” in *Vehicular Technology Conference, 2007. VTC2007-Spring. IEEE*, Apr. 2007, pp. 1234–1238.
[17] H. Holma and A. Toskala, *LTE for UMTS: OFDMA and SC-FDMA Based Radio Access*. Chichester, UK: Wiley, 2009.
[18] T. Beniero, S. Redana, J. Hamalainen, and B. Raaf, “Effect of relaying on coverage in 3GPP LTE-Advanced,” in *Vehicular Technology Conference, IEEE*, Apr. 2009.
[19] S. Tombaz, A. Vastberg, and J. Zander, “Energy and cost efficient ultra-high capacity wireless access,” in *IEEE Green Net Workshop*, May 2011.
[20] A. Lozano, A. M. Tulino, and S. Verdu, “Optimal power allocation for parallel gaussian channels with arbitrary input distributions,” in *Info. Theory, IEEE Trans. on*, vol. 52, July 2006, pp. 3033–3051.
[21] H. Yousefizadeh and H. Jafarkhani, “An optimal power-throughput tradeoff study for mimo fading ad-hoc networks,” in *KICS Journal of Communications and Networks*, vol. 12, Aug. 2010, pp. 334–346.
[22] T. A. Le and M. R. Nakhai, “Possible power saving gains in dividing a cell into tiers of smaller cells,” in *IET Electronics Letters*, Aug. 2010, pp. 1163–1165.
[23] F. Cao and Z. Fan, “The tradeoff between energy efficiency and system performance of femtocell deployment,” in *Proc. International Symposium on Wireless Communication Systems (ISWCS)*, Nov. 2010.
[24] A. Dinnis and J. Thompson, “The effects of including wraparound when simulating cellular wireless systems with relaying,” in *Vehicular Technology Conference, IEEE*, Apr. 2007, pp. 914–918.
[25] P. Kyosti, J. Meinila, L. Hentila, and X. Zhao, “WINNER II Channel Models: Part I Channel Models version 1.2,” WINNER and Information Society Technologies,” Technical Report, 2007.
[26] 3GPP, “TR36.814 V9.0.0: Further Advancements for E-UTRA Physical Layer Aspects (Release 9),” 3GPP,” Technical Report, Mar. 2010.
[27] EARTH, “WP2.D2.3: Energy Efficiency Analysis of the Reference Systems,” Energy Aware Radio and Network Technologies (EARTH),” Technical Report, Dec. 2010.
[28] C. Mehlfuhrer, M. Wrulich, J. Ikuno, D. Bosanska, and M. Rupp, “Simulating the long term evolution physical layer,” in *European Signal Processing Conference, EURASIP*, Aug. 2009, pp. 1471–1478.
[29] G. Auer, V. Giannini, I. Godor, P. Skillermark, M. Olsson, M. Imran, D. Sabella, M. Gonzalez, C. Desset, and O. Blume, “Cellular energy efficiency evaluation framework,” in *Vehicular Technology Conference (VTC Spring), 2011 IEEE*, May 2011, pp. 1–6.
[30] M. Haenggi, J. G. Andrews, F. Baccelli, O. Dousse, and M. Franceschetti, “Stochastic geometry and random graphs for the analysis and design of wireless networks,” in *Selected Areas in Communications (JSAC), IEEE Journal on*, vol. 28, Sept. 2009, pp. 1029–1046.
[31] J. N. Laneman, G. W. Wornell, and D. N. C. Tse, “Cooperative diversity in wireless networks: Efficient protocols and outage behaviour,” in *IEEE Trans. on Inform. Theory*, Dec. 2004, pp. 3062–3080.

Weisi Guo received his B.A., M.Eng., M.A. and Ph.D. degrees from the University of Cambridge. He is currently at the University of Sheffield and is the author of the VCESIM LTE Dynamic System Simulator. His research interests are in the areas of self-organizing, energy-efficient, and multi-user cooperative wireless networks.

Tim O’Farrell holds a Chair in Wireless Communication at the University of Sheffield, UK. He is the Academic Coordinator of the MVCE Green Radio Project. His research encompass resource management and physical layer techniques for wireless communication systems. He has led over 18 research projects and published over 200 technical papers including 8 granted patents.